Received: 24 March 2020 | Revised: 17 June 2020 | Accepted: 26 June 2020

DOI: 10.1002/aoc.5935

FULL PAPER

Applied Organometallic Chemistry WILEY

Ligand directed synthesis of a unprecedented tetragonalbipyramidal copper (II) complex and its antibacterial activity and catalytic role in oxidative dimerisation of 2-aminophenol

Shreya Mahato[1] | **Nishith Meheta**[1] | **Muddukrishnaiah Kotakonda**[2] | **Mayank Joshi**[3] | **Prasanta Ghosh**[4] | **Madhusudan Shit**[5] | **Angshuman Roy Choudhury**[3] | **Bhaskar Biswas**[1]

[1]Department of Chemistry, University of North Bengal, Darjeeling-734013, India

[2]Department of Pharmaceutical Technology, Anna University, BIT Campus Thiruchirappalli, India

[3]Department of Chemical Sciences, Indian Institute of Science Education and Research, Mohali, Sector 81, Knowledge City, S. A. S. Nagar, Manauli PO, Mohali, Punjab 140306, India

[4]Department of Chemistry, Narendrapur Ramakrishna Mission Residential College, Kolkata 700103, India

[5]Department of Chemistry, Dinabandhu Andrews College, Kolkata 700084, India

Correspondence
Bhaskar Biswas, Department of Chemistry, University of North Bengal, Darjeeling-734013, India.
Email: icbbiswas@gmail.com

Funding information
Science and Engineering Research Board, Grant/Award Number: TAR/2018/000473

In pursuit of the significant contribution of copper ion in different biological processes, this research work describes the synthesis, X-ray structure, Hirshfeld surface analysis, oxidative dimerization of 2-aminophenol and antibacterial activity of a newly designed copper (II)-Schiff base complex, $[Cu(\mathbf{L})_2]$ (1), [Schiff base (H**L**) = 2-(2-methoxybenzylideneamino)phenol]. X-ray structural analysis of 1 reveals that the Cu (II) complex crystallizes in a cubic crystal system with *I*a-3d space group. The Cu (II) centre adopts an unprecedented tetragonal bipyramidal geometry in its crystalline phase. The Schiff base behaves as a tridentate chelator and forms an innermetallic chelate of first order with Cu (II) ion. The copper (II) complex has been tested in the bio-mimics of phenaxozinone synthase activity in acetonitrile and exhibits good catalytic activity as evident from high turnover number, 536.4 h^{-1}. Electrochemical analysis exhibits the appearance of two additional peaks at −0.15 and 0.46 V for Cu (II) complex in presence of 2-AP and suggests the development of $AP^{-}/AP^{\bullet -}$ and $AP^{\bullet -}$/IQ redox couples in solution, respectively. The presence of iminobenzosemiquinone radical at g = 2.057 in the reaction mixture was confirmed by electron paramagnetic resonance and may be considered the driving force for the oxidative dimerisation of 2-AP. The existence of a peak at m/z 624.81 for Cu (II) complex in presence of 2-AP in electrospray ionization mass spectrum ensures that the catalytic oxidation proceeds through enzyme-substrate adduct formation. The copper (II) complex exhibits potential antibacterial properties against few pathogenic bacterial species like *Staphylococcus aureus*, *Enterococcus* and *Klebsiella pneumonia* and scanning electron microscope studies consolidates that destruction of bacterial cell membrane accounts on the development of antibacterial activity.

Shreya Mahato and Nishith Meheta have equal contribution.

KEYWORDS

aminophenol oxidation activity, antibacterial property, copper (II), electrochemical analysis, X-ray structure

1 | INTRODUCTION

In this modern age of science, Schiff base as polydentate chelators have been widely used in the development of coordination compounds of varied functionality.[1–3] Among the transition metal ions, copper ion has been considered as an essential metal ion in living system and it also plays significant role in designing advance functional materials.[4–7] In nature, copper ions are integrated with different bio-ligands in the functional sites of various metallo-enzymes such as catechol and galactose oxidase, phenoxazinone synthase, superoxide dismutase, lysine oxidase, N_2O reductase etc.[8–11] It pursuit of deep understanding of different biological oxidation processes in nature, synthetic coordination chemists have been stepped forward to tune electronic and geometric factors of the ligands in engineering bio-inspired coordination driven compounds.[12–15] It is well documented that the bio-inspired synthetic analogues also serve as magic catalysts in several catalytic oxidation reactions of laboratory and industrial significance.[14–16] Among the different oxidase enzymes, phenoxazinone synthase has drawn special attention[14,15] as the oxidized product, aminophenoxazinone acts as an antineoplastic agent named actinomycin D (questiomycin A) which is usually recommended in the treatment of certain types of cancer.[17–20] Furthermore, 2-aminophenoxazin-3-one and 3-aminophenoxazin-2-one compounds show potential antimicrobial, antiviral, and antitumor activities against different pathogens.[21–24] Aminophenoxazinone compounds have also been reported in different forms like Streptomyces parvulus and wood rotting fungi metabolites, oxidative coupling products of o-aminophenols with bovine erythrocyte hemolyzate, and bio-conversion products of Pseudomonas putida grown on nitroarenes.[24–28]

In light of incessant emergence for new antibiotics with potential resistance against microorganisms, it is of great importance to design novel antibiotics, which would destroy the lipoid layer as well as the cell membrane of the pathogen with high selectivity.[29,30] In this perspective, copper based coordination compounds hold a great promise to provide future alternatives to the existed antibiotics.[30,31] In the context of newly designed copper (II) complexes with high catalytic activities and potential therapeutic values, this research study deals with the synthesis, structural characterization and catalytic oxidase activity of a new copper (II)-Schiff base complex. The antibacterial property of this copper (II) complex towards different bacterial species has also been delineated.

2 | EXPERIMENTAL

2.1 | Preparation of the Schiff base and dinuclear copper (II) complex

2.1.1 | Chemicals, solvents and starting materials

Highly pure *o*-anisidine (Sigma Aldrich, Missouri, Texas, USA), salicylaldehyde (Sigma Aldrich, Missouri, Texas,USA) and cupric acetate monohydrate (SRL, Gurugram, Haryana, India) were purchased from the respective concerns and used as received. All other chemicals and solvents were of analytical grade and used as received without further purification.

2.1.2 | Synthesis of the Schiff base and copper (II) complex

The Schiff base, H**L** was synthesized following a reported method.[32] The Schiff base was synthesized through condensation reaction between *o*-anisidine (0.123 g, 1 mmol) and salicylaldehyde (0.122 g, 1 mmol) in ethanol under reflux for 8 hr. Then, the yellowish brown coloured gummy product was extracted and stored *in vaccuo* over $CaCl_2$ for use. Yield: 0.201 g (∼88.5%). Anal. Calc. for $C_{14}H_{13}NO_2$ (H**L**): C, 73.99; H, 5.77; N, 6.16; Found: C, 73.93; H, 5.72; N, 6.19. IR (KBr, cm^{-1}; Figure S1): 3372 (ν_{OH}), 1615, 1590 ($\nu_{C=N}$); UV–Vis (λ_{max}, nm; Figure S2): 230, 270, 346; ^1H NMR (δ ppm, 400 Mz, $CDCl_3$; Figure S3) δ = 13.88 (s, 1H), 8.63 (s, 1H), 7.26–6.82 (Ar-H, 7H), 3.79–3.83 (t, 3H) ppm. ^{13}C NMR (400 MHz,$CDCl_3$; Figure S4): 162.06 (HC=N); 153.03, (Ar-OH); 137.05 (Ar-N=C); 132.94, 132.05, 127.95, 127.13, 119.64, 118.46, 117.40, 115.05, (Ar-C); 77.49, 77.17, 76.85 (-OCH_3).

The copper (II)-Schiff base complex was prepared by drop wise addition of acetonitrile solution of Cu $(OAc)_2$ (0.199 g, 1 mmol) to the methanolic solution of H**L** (0.454 g, 2 mmol). The yellow coloured Schiff base solution was instantly turned to green coloured solution.

Thereafter, the reaction mixture was kept on a magnetic stirrer for 20 mins and kept in open atmosphere for slow evaporation. After 7–10 days, green coloured single crystals of the compound were separated out from the solution. The crystalline compound was washed with toluene and dried over silica gel. Finally, different spectroscopic analysis was carried out to determine the structural formulation of the Cu (II)-Schiff base complex. The results are summarized as follows.

Yield of **1**: 0.415 g (∼63.5% based on metal salt) Anal. calc. For $C_{28}H_{24}N_2O_4Cu$ (**1**): C, 65.17; H, 4.69; N, 5.43; Found: C, 65.13; H, 4.61; N, 5.38. IR (KBr pellet, cm^{-1}; Figure S1): 1605,1585 ($\nu_{C=N}$); UV–Vis (1×10^{-4} M, λ_{max} (abs), nm, MeCN; Figure S2): 238, 283, 400.

2.2 | Physical measurements

FTIR-8400S SHIMADZU spectrometer (Shimadzu, Nakagyo-ku, Kyoto, Japan) was employed to record IR spectrum (KBr) of Schiff base and **1** in the range of 400–3,600 cm^{-1}. ^1H and ^{13}C NMR spectra of the ligand (H**L**) were obtained on a Bruker Advance 400 MHz spectrometer (Bruker, MA, USA) in $CDCl_3$ at 298 K. Steady-state absorption and other spectral data were recorded with a JASCO V-730 UV–Vis spectrophotometer (Jasco, Hachioji,Tokyo, Japan). Electrospray ionization (ESI) mass spectral measurements were performed with a Q-TOF-micro quadruple mass spectrometer (Waters, Milford,USA). Elemental analyses were performed on a Perkin Elmer 2400 CHN microanalyser (Perkin Elmer, Waltham, Massachusetts, USA). X-band EPR spectra were recorded on a Magnettech GmbH MiniScope MS400 spectrometer (equipped with temperature controller TC H03, Magnettech, Berlin, Germany), where the microwave frequency was measured with an FC400 frequency counter. The EPR spectrum of Cu (II) complex was simulated using Easy Spin software.

2.3 | Crystal structure determination and refinement

X-ray diffraction data of **1** were collected using a Rigaku XtaLABmini diffractometer equipped with Mercury 375R (2 × 2 bin mode) CCD detector. The data were collected with graphite monochromated Mo-Kα radiation (λ = 0.71073 Å) at 296 (2) K using ω scans. The data were reduced using CrysAlisPro 1.171.39.35c[33a] and the space group determination was done using Olex2. The structure was resolved by dual space method using SHELXT-2015[33b] and refined by full-matrix least-squares procedures using the SHELXL-2015[33c] software package through OLEX2 suite.[33d]

2.4 | Hirshfeld surface calculations of copper (II) compound

Crystal Explorer 17.5[34a] progam package was employed to generate Hirshfeld surfaces[34b] and 2D fingerprint plots[34c] of **1** using its single crystal X-ray diffraction data. Hirshfeld Surface analysis is an important tool to study and locate intermolecular interactions within crystal packing.[34c,d] The function d_{norm} is a ratio of the distances of any surface point to the nearest interior (d_i) and exterior (d_e) atom, and the van der Waals radii of the atoms.[35,36] The normalized contact distance (d_{norm}) could be expressed following the equation 1.

$$d_{norm} = \frac{d_i - r_i^{vdW}}{r_i^{vdW}} + \frac{d_e - r_e^{vdW}}{r_e^{vdW}} \quad (1)$$

Where, r_e^{vdW} and r_i^{vdW} denote the corresponding van der Waals radii of atoms. The negative value of d_{norm} indicates that the sum of d_i and d_e is shorter than the sum of the relevant van der Waals radii, which is considered to be a closest contact and is visualized in red colour. The white colour denotes intermolecular distances close to van der Waals contacts with d_{norm} equal to zero whereas contacts longer than the sum of van der Waals radii with positive d_{norm} values are coloured with blue. A plot of d_i versus d_e is a fingerprint plot that identifies the presence of different types of intermolecular interactions.

2.5 | Aminophenol oxidation activity of copper (II) complex (1)

Aminophenol oxidation activity was studied by treating 1×10^{-4} M solution of Cu (II) complex with 1×10^{-3} M of 2-aminophenol (2-AP) solution in acetonitrile under aerobic conditions at room temperature. Absorbance vs. wavelength (wavelength scans) of the solution was monitored through spectrophometer at a regular time interval of 6 min for 1 hr in the wavelength range from 300–700 nm.[13,15]

Kinetic experiments were also carried out spectrophotometrically to specify the efficacy of catalytic oxidation of aminophenol by the Cu (II) complex in MeCN at 298 K.[13,15] 0.04 ml of the complex solution with a constant concentration of 1×10^{-4} M was added to 2 ml solution of 2-AP of a particular concentration (varying its concentration from 1×10^{-3} M to 1×10^{-2} M) to achieve the ultimate concentration as 1×10^{-4} M. The conversion

of 2-aminophenol to 2-aminophenoxazine-3-one was monitored with time at a wavelength 407 nm (time scan) in MeCN.[13,15,37,38] To determine the dependence of rate on substrate concentration, kinetic analyses were performed in triplicate.

The oxidized product was extracted by column chromatography. Neutral alumina was employed as column support and benzene-ethyl acetate solvent mixture was treated as an eluant mixture in this chromatographic separation. The purity of catalytic oxidation product of 2-AP was examined by proton NMR spectroscopy. ^{1}H NMR spectral analysis reveals to identify the final product. ^{1}H NMR data for 2-amino-3*H*-phenoxazine-3-one (APX), ($CDCl_3$, 400 MHz,) δ_H: 7.61 (m, 1H), 7.45 (m, 3H), 6.46 (s, 1H), 6.37 (s, 1H), 6.25 (s, 1H).

2.6 | Detection of presence of hydrogen peroxide in the catalytic oxidation of 2-aminophenol

The involvement of aerobic oxygen in the course of oxidative dimerization of 2-AP was examined by testing the presence of hydrogen peroxide following a reported procedure.[37,38] In the oxidation of aminophenol in MeCN, the solution was acidified with H_2SO_4 till the pH of the solution became 2. After a certain time, an equal volume of water was added to stop further oxidation. The phenoxazinone species were extracted three times with dichloromethane. 1 ml of 10% solution of KI and three drops of a 3% solution of ammonium molybdate were added to the aqueous layer. The formation of I_3^- was monitored through spectrophotometer to examine the development of the characteristic I_3^- band (λ_{max} = 353 nm) which may be assignable to the production of hydrogen peroxide.

2.7 | Electro-chemical analysis

The electroanalytical instrument, BASi Epsilon-EC was employed for electrochemical experiments in CH_2Cl_2 solutions containing 0.2 M tetrabutylammonium hexafluorophosphate as supporting electrolyte. The BASi platinum working electrode, platinum auxiliary electrode, Ag/AgCl reference electrode were used for the measurements.

2.8 | Antimicrobial susceptibility studies

Antibacterial activity of the Cu (II) complex was tested against few clinical pathogenic bacteria by well plate and serial dilution method.

2.8.1 | Bacterial strains (clinical bacterial cultures), culture media

The antimicrobial property of the Cu (II) complex was examined against clinical *Staphylococcus aureus*, *Enterococcus* and *Klebsiella.* Microbial cultures were procured from government medical college from Tiruchirappalli, Tamil Nadu. Muller-Hinton agar media of Himedia Pvt. Bombay, India was used for the media for the microbial test. The antibacterial activity was evaluated by using the Himedia zone reader.

2.8.2 | Agar well diffusion method

The antibacterial activity of Cu (II)-Schiff base complex and a standard drug (Amikacin-100 mg/2 ml) was studied initially by using a well plate method. *Staphylococcus aureus*, *Enterococcus* and *Klebsiella pneumoniae* inoculums were prepared by using nutrient broth media. Double strength sterile Mueller Hinton agar media were prepared by autoclaving 7.6 gm in 100 ml. Inoculate the test microorganisms on the Mueller Hinton agar plates by using sterile cotton swabs. Formulations of Cu (II) complex and Amikacin were placed on agar well. Plates were incubated for 30 min at the refrigerator to diffuse the formulation into the agar plate, and finally, plates were again incubated at 37°C for 24 hr. Antibacterial activity was evaluated by using the Himedia zone reader.

2.8.3 | Determination of MIC and MBC for Cu (II) complex against clinical *Klebsiella pneumoniae*

The minimum inhibitory concentration (MIC) and minimum bactericidal concentration (MBC) was determined by selecting *Klebsiella pneumonia.* Among the three pathogenic bacteria, *Klebsiella pneumoniae* is a very well-known opportunistic pathogen that accounts for ~10% of nosocomial bacterial infections, including sepsis, pneumonia, urinary tract infections, and hepatic abscess. The organism can invade almost all part of the human body, although the most frequently affected urinary and respiratory tracts.

The method of micro-dilution was used to establish the antibacterial potential of the copper (II)-Schiff base complex and respective controls. A spectrophotometer (OD595 = 0.22) equivalent to 10^8 CFU/mL used to fix the bacterial cultures to 0.22 optical density at 595 nm. Different concentrations of Cu (II) complex and the respective controls in 2.0 ml centrifuge tubes at 37°C for

2 hr, were incubated with an inoculum of 10 μL of the above bacteria culture. Next, bacteria were diluted serially and placed 10 μL of each dilution on nutrient agar plates. Such plates were incubated overnight at 37°C, followed by a viable count of CFU bacteria.[39]

Preparation of stock solutions for MIC was done according to following equation 2.

$$\begin{aligned} &Weight\ of\ the\ powder\ (mg) \\ &= \frac{Volume\ of\ solution\ (mL) \times Concentration\ (mg/L)}{The\ potency\ of\ powder\ (mg/g)} \end{aligned} \quad (2)$$

2.8.4 | Antimicrobial activity of Cu (II) complex using scanning electronic microscope

To examine the mode of action of Cu (II) complex on bacterial species, bacterial cultures were obtained from MIC and MBC samples and centrifuged. Thereafter, the bacterial cells were collected and sputter-coated with a thin layer of gold–palladium. The coated bacterial cells were fixed on a glass coverslip and observed under a scanning electron microscope.[40]

3 | RESULTS AND DISCUSSION

3.1 | Synthesis and formulation of the Schiff base (HL) and copper (II) complex(1)

The tridentate Schiff base was prepared by refluxing *o*-aminophenol with *o*-anisaldehyde in 1:1 mole ratio in ethanol. The synthetic route is given in Scheme 1. The Cu (II) complex was synthesized by adding copper (II) acetate to H**L** in 2:3 mole ratio in methanol-acetonitrile under slow stirring on magnetic stirrer. Different ratio of Cu (II) acetate and H**L** was also used to produce copper (II) complex of varied nuclearity, however same molecular composition,$[Cu(\mathbf{L})_2]$ was observed in each cases. Replacement of copper (II) acetate by hydrated copper (II) chloride also produced same Cu (II) complex. Single crystal form of the Cu (II) complex was obtained by slow evaporation of reaction mixture at room temperature. This Cu (II) complex is highly soluble in polar solvents like methanol, acetonitrile, chloroform etc.

3.2 | Description of crystal structure

X-ray structural analysis indicates that the Cu (II) complex crystallizes in a cubic crystal system with *I*a-3d space group. The thermal ellipsoidal plot of Cu (II) complex is shown in Figure 1. The structural refinement parameter for this Cu (II) complex is presented in Table 1. The bond angles and bond distances are given in Table 2. Two units of H**L** coupled with one Cu (II) ion and lead to mononuclear Cu (II) complex of inner-metallic chelate of first order. In accordance with the disposition of coordination centres around metal centre as well as M-L bond angle values, it is confirmed that the Cu (II) centre adopts an irregular six coordinate geometry. The coordination geometry of copper (II) ion is described as tetragonal bipyramidal geometry. Close inspection on coordination geometry suggests that Cu (II) centre forms a tetragonal plane based on O1,O1, N1,O2 and bipyramidal geometry appears from apical existence of two donor sites, N1 and O2.

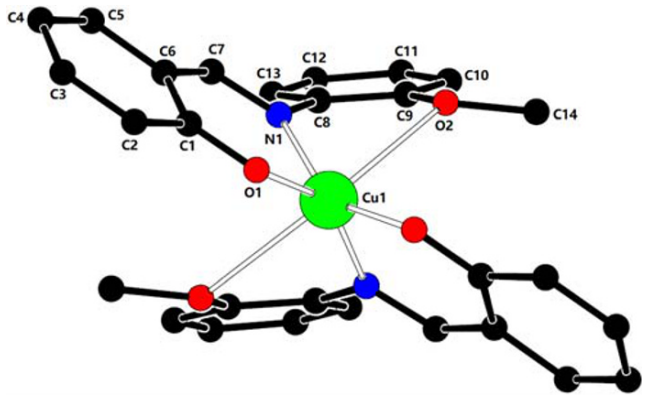

FIGURE 1 X-ray structure of the copper (II)-Schiff base complex with 30% ellipsoid probability

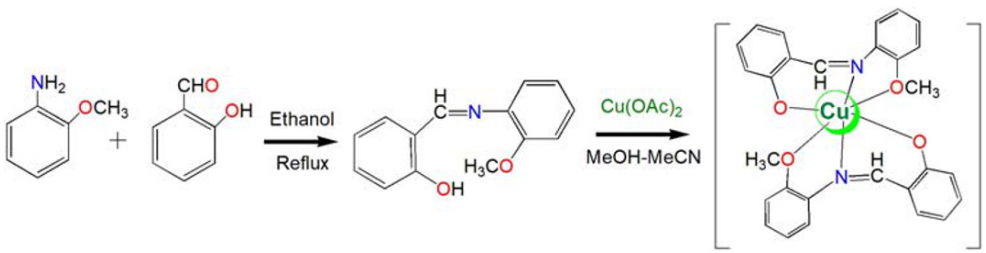

SCHEME 1 Synthetic route for the formation of 1

TABLE 1 Crystallographic data and structure refinement parameters for **1**

Parameters	1
Empirical formula	$C_{28}H_{24}N_2O_4Cu$
Formula weight	516.03
Temperature (K)	296
Crystal system	Cubic
Space group	*I*a-3d
a (Å)	31.2952(17)
b (Å)	31.2952(17)
c (Å)	31.2952(17)
Volume (Å^3)	30,650(3)
Z	48
ρ (gcm^{-3})	1.571
μ (mm^{-1})	0.890
F (000)	12,816
R_{int}	0.179
θ ranges (°)	2.4–32.9
Number of unique reflections	4,617
Total number of reflections	69,708
Final R indices	0.0984, 0.3585
Largest peak and hole (eA°$^{-3}$)	1.38, −0.34

TABLE 2 Bond angles and bond distances value of Cu (II) complex

Bond distances			
Cu1-O1	**1.903(4)**	**Cu1-O2**	**2.727(4)**
Cu1-N1	1.981(4)	Cu1-O1a	1.903(4)
Cu1-O2a	2.727(4)	Cu1-N1a	1.981(4)
Bond angles		O11-Fe2-O3	94.9(3)
O1-Cu1-O2	128.81(15)	O1-Cu1-N1	93.62(17)
N1-Cu1-O1a	88.84(18)	O1-Cu1-O2a	88.74(15)
O1-Cu1-N1a	149.01(17)	O2-Cu1-N1	65.86(14)
O1a-Cu1-O2	88.74(15)	O2-Cu1-O2a	129.91(11)
O2-Cu1-N1a	82.15(14)	O1a-Cu1-N1	149.01(17)
O2a-Cu1-N1	82.15(14)	N1-Cu1-N1a	99.77(16)
O1a-Cu1-O2a	128.81(15)	O1a-Cu1-N1a	93.62(17)
O2a-Cu1-N1a	65.86(14)		

3.3 | Hirshfeld analysis of copper (II)-Schiff base complex

Crystal Explorer software was employed to demonstrate the Hirshfeld surface of Cu (II) complex (Figure S5) over a definite d_{norm}. The surface volume is calculated as 628.31 Å^3 and surface area is determined as 491.0 Å^2. The red highlighted area shows the d_{norm} area and close non-covalent interactions of **1** with its surrounding within the 3D crystal. Percentage share of each element in close interaction with others is given in Table S1. In this d_{norm}, the blue area is showing the weak C-H···π interactions between aromatic H attached to aromatic C and aromatic rings of the ligands. Red area indicates very weak intermolecular C-H···O H-bonding between C-H of benzene ring and O of OPh/OCH_3. This molecule is interacted by surrounding molecules through C-H···O hydrogen bond, and C-H···π interactions as display in Fingerprint plots (Figure S6). Quantitative information of different intermolecular interactions by each pair of elements is given in Table S1.

3.4 | Solution property of the Schiff base and copper (II) complex

The electronic transitions for the Schiff base and its Cu (II) complex were recorded in acetonitrile medium (MeCN) from 200 to 900 nm at room temperature. The Schiff base, H**L** displayed electronic transitions at 230, 270 nm and 346 nm and the Cu (II) complex exhibited electronic bands at 238, 283 and 400 nm. The electronic spectra are displayed in Figure S2. Electronic bands at 230, 270 and 346 nm in the UV region for the Schiff base may be attributed to π → π* and n → π* electronic transitions.[41] The appearance of electronic bands at 238 and 283 nm may be corresponded to π → π* and n → π* electronic transitions of ligand origin[41] while the optical band at 400 nm may be assigned as phenoxo to Cu (II) ion electronic transition.[42b,c]

The electrolytic behaviour of the Cu (II) complex has been checked through measurement of molar conductivity in MeCN medium at room temperature. The molar conductance value was recorded for 1.15 × 10^{-3} M solution of **1** as 05 Sm^{2}mol^{-1}. The molar conductance value suggests about the non-electrolytic nature of the Cu (II) complex in MeCN medium.[43]

3.5 | Phenoxazinone synthase mimicking activity of the copper (II) complex (1)

The oxidation of 2-aminophenol (2-AP) was studied by addition of catalytic amount of copper (II) complex (1 × 10^{-4} M) to 2-AP (1 × 10^{-3} M) under aerobic atmosphere at 25°C (Scheme 2).

The changes of absorbance in the course of catalysis were monitored through a UV–Vis spectrophotometer. The wavelength scan was recorded for 1 hr with a time

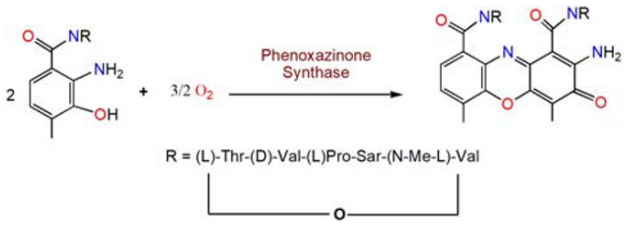

SCHEME 2 Catalytic oxidation of substituted aminophenol by phenoxazinone synthase

interval of 5 min (Figure 2). The substrate, 2-AP exhibits a characteristic single electronic transition at 267 nm in MeCN and indicates its high purity in solution. Addition of the solution of Cu (II) complex to the solution of 2-AP in MeCN, the optical band corresponding to phenoxo to Cu (II) electronic transition at 400 nm was initiated to exhibit a bathochromic shift. As a result, a new electronic band at 407 nm with increasing absorbance was developed (Figure 2). Switching of the electronic band from 400 nm to 407 nm is a definite signature for the oxidation of 2-AP in MeCN.[13,15,44] This spectrophotometric evidence may correspond to the development of aminophenoxazinone species in solution.

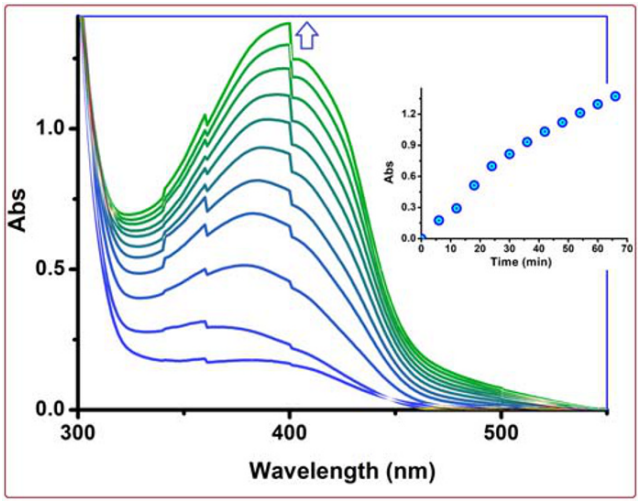

FIGURE 2 Development of new electronic band at 407 nm upon addition of Cu (II) complex to of 2-AP in MeCN. (The spectra are recorded after every 6 min). Inset: Time vs Absorbance plot at defined wavelength

The kinetics for the oxidative coupling of 2-AP was also carried out to understand the catalytic efficacy of the copper (II) catalyst. The method of initial rates was followed to unveil the kinetic parameter of this oxidative dimerization of 2-AP. The growth of oxidation product was monitored at 407 nm as a function of time (Figure S7).[13,15,37,38,44] The rate constants vs. substrate concentration displayed the nature of kinetics (Figure S7). The first order saturation kinetics reveals that Michaelis–Menten model seems to be applicable in this case and may be presented according to the following equation 3:

$$V = \frac{V_{\max}[S]}{K_M + [S]} \quad (3)$$

Where, V is rate of the reaction, K_m is denoted as Michaelis–Menten constant, $V_{\max}$ is the maximum velocity of the reaction, and $[S]$ is concentration of the substrate.

The values of kinetics parameters were determined from Michaelis–Menten equation as V_{max} (MS^{-1}) = 1.49×10^{-5}; $K_M = 9.46 \times 10^{-4}$ [Std. Error for V_{max} (MS^{-1}) = 2.55×10^{-6}; Std. Error for K_m (M) = 1.72×10^{-5}].

A comparison of catalytic oxidation of 2-AP by this Cu (II) complex with some other reported Cu (II) complexes is tabulated in Table 3.[26c,45–47] The catalytic efficiency for the oxidative dimerization of 2-AP by this Cu (II) complex was found high as $k_{cat}/K_M = 5.67 \times 10^5$.

TABLE 3 Comparison of k_{cat} (h^{-1}) values for catalytic oxidation of 2-AP by reported copper (II) compounds and **1**

Complex	k_{cat} (h^{-1})(Solvent)	CCDC No	Ref
$[L^1Cu(\mu\text{-}Cl)_2CuL^1]$	1,065 (CH_3OH)	1,572,023	[45]
	213 (CH_3CN)		
$[Cu_4(L^2)_4]$	86.3 (CH_3OH)	1,507,035	[46]
$[Cu_4(L^3)_4]$	340.26 (CH_3OH)	1,507,036	[46]
$[Cu_2(L^4)_3]$	78.14 (CH_3OH)	1,957,033	[26c]
$[Cu(2,2'\text{-bpy})Cl_2]$	2.08×10^3(CH_3OH)	1,524,681	[15c]
$[Cu(2,2'\text{-bpy})_2(OAc)]^+$	1.83×10^3 (CH_3OH)	1,513,638	[47]
$[Cu(\mathbf{L})_2]$	5.364×10^2 (CH_3CN)	1,957,033	This work

L^1 = 2-(a-Hydroxyethyl)benzimidazole (Hhebmz), L^2 = (E)-4-Chloro-2-((thiazol-2-ylimino)methyl)phenol, L^3 = (E)-4-Bromo-2-((thiazol-2-ylimino)methyl)phenol, L^4 = (Z)-2-methoxy-6-(((2-methoxyphenyl)imino) methyl)phenol].

Electrochemical analysis and EPR studies were vperformed to understand the catalytic behaviour of Cu (II) complex in the oxidative dimerization of 2-AP in acetonitrile medium. The cyclic voltammogram of the Cu (II) complex was recorded in dichloromethane medium at 298 K where N-tetrabutylammonium hexafluorophosphate was employed to record the electrochemical data in aerobic environment and shown in Figure 3. The Cu (II)-Schiff base complex displays one irreversible cathodic wave at −0.94 V which is assignable to electron transfer in Cu^{2+} to Cu^{+} redox couple in solution phase. The active participation of copper (II) centre in catalytic oxidation of 2-AP is confirmed by measurement of redox potentials of Cu (II) complex in presence of 2-AP under identical reaction conditions.

The mixture of copper (II) complex in presence of 2-AP produces irreversible cathodic peak at −1.11 V due to Cu^{2+} to Cu^{+} redox couple i.e. the peak shifted from −0.94 to −1.11 V due to co-ordination of 2- AP to the Cu^{2+} centre of the complex. Furthermore, two new peaks at −0.15 and 0.46 V appeared which were assigned to the development of $AP^{-}/AP^{\bullet -}$ and $AP^{\bullet -}/IQ$ redox couples. The redox potential data strongly suggests the course of 2-AP oxidation undergoes through iminobenzoquinone radical formation. To view more insights of this copper (II) complex mediated oxidative coupling of 2-AP, EPR spectra of the Cu (II) complex in presence and absence of 2-AP are recorded in MeCN and presented in Figure 4.

The EPR spectrum of copper (II) complex (**1**) with X-band frequency at room temperature in MeCN medium displays four line hyperfine spectra at g = 2.12 due to presence of ^{63}Cu nuclei with $I = 3/2$.[13,15] and the calculated EPR spectrum for the Cu (II)-Schiff base resembles very well as evident from the simulated g value, 2.1262 (Figure 4). The mixture of copper complex in presence of 2-AP is EPR silent due to antiferromagnetic coupling

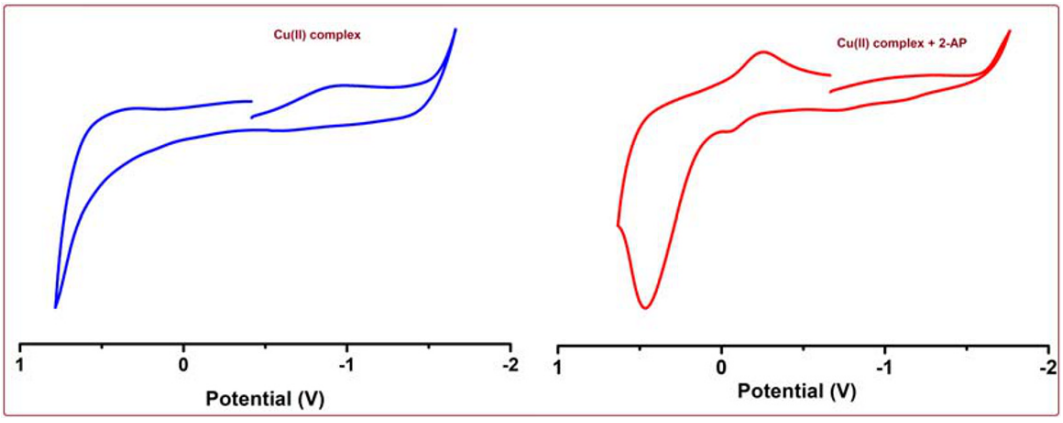

FIGURE 3 Left: Cyclic voltammogram of the Cu (II)-Schiff base complex in anhydrous DCM medium; Right: Cyclic voltammogram of Cu (II) complex in presence of 2-AP under molecular oxygen atmosphere in anhydrous DCM in CH2Cl2 (0.20 M [N(n − Bu)4]PF6) at 295 K

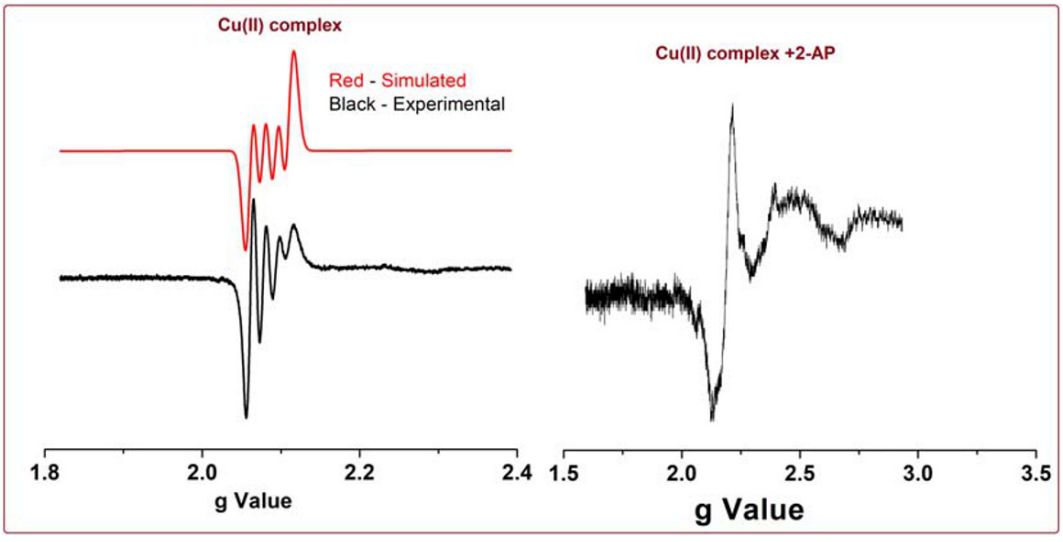

FIGURE 4 X- band EPR spectra of the copper (II)-Schiff base in presence of 2-AP after 20 min in CH3CN solution at 298 K

between Cu^{2+}(S = 1/2) with iminobenzosemiquinonate anion radical. The EPR spectral analysis of the copper complex in presence of 2-AP in acetonitrile at room temperature strongly suggests the generation of radical species for the appearance of additional signal at g ca 2.057 (Figure 4). The reported g value for oxidised 2-AP radical (iminobenzoquinone) is 2.0051 in 10^{-1} M Bu_4NPF_6.[15c,26]

Furthermore, electrospray ionization (ESI) mass spectrum of the copper (II)-Schiff base complex in presence of 2-AP is recorded after mixing of 10 min to reveal the binding aspects of the copper (II) complex and 2-AP. It was observed that the ESI-Ms of the reaction mixture (Figure S8) exhibits the base peak at m/z 213.12 which is assignable to the presence of aminophenoxazinone species, [(2-amino-3*H*-phenoxazine-3-ones) + H^+]. Appearance of another important peak at m/z 624.81 corresponds to the formation of adduct between copper (II)-Schiff base complex and 2-AP, [[**1** + (2-AP)] + H^+]. The experimental m/z values correlate well with the theoretical m/z values. In this context, involvement of molecular oxygen in the course of oxidation of 2-AP was tested through production of hydrogen peroxide in solution using a reported method.[37,38] No spectral band at λ_{max} 353 nm corresponds to generation of hydrogenperoxide was observed throughout the course of catalysis and ensure the presence of water as a byproduct appeared from molecular oxygen.

Previously study by P. Chaudhury and co-workers[48] presented tetracopper complex as a bio-mimetic model towards 2-AP oxidation and recommends an "on–off" mechanism via radical generation in active participation with the metal centres favouring 6e oxidative coupling of substrate. T.P. Begley and co-workers[49] suggests the production of 2-aminophenoxazinone through a sequence of three consecutive 2e oxidation of 2-AP. The tautomerization reactions were the controlling unit in regeneration of the 2-Ap during this course of catalytic oxidation reaction. Based upon the outcomes observed by different analytical methods like electrochemical, EPR and ESI-MS, a plausible mechanism is proposed in Scheme 3. So, oxidative dimerization of 2-AP undergoes through formation of catalyst-substrate intermediate in the primary stage. Subsequently, Cu centre activates molecular oxygen to produce water as a byproduct and iminobenzosemiquinonate radical in the course of catalytic oxidation. Iminobenzosemiquinonate radical proceeds to couple with another unit of 2-AP and develop aminophenoxazinone species as a final product.

3.6 | Antibacterial activity of the cu (II)-Schiff base complex

The antibacterial activity of Cu (II) complex was assessed through the method of well diffusion against the bacteria *Staphylococcus aureus*, *Enterococcus* and *Klebsiella pneumoniae*. The results of the inhibition zone diameters shown in Table S2. The therapeutic efficiency of this Cu (II) complex was determined by calculating MIC and MBC on *Klebsiella pneumoniae* (Table S3). *MIC and MBC* values were determined as 1.250 mg/ml, 0.625 mg/ml for

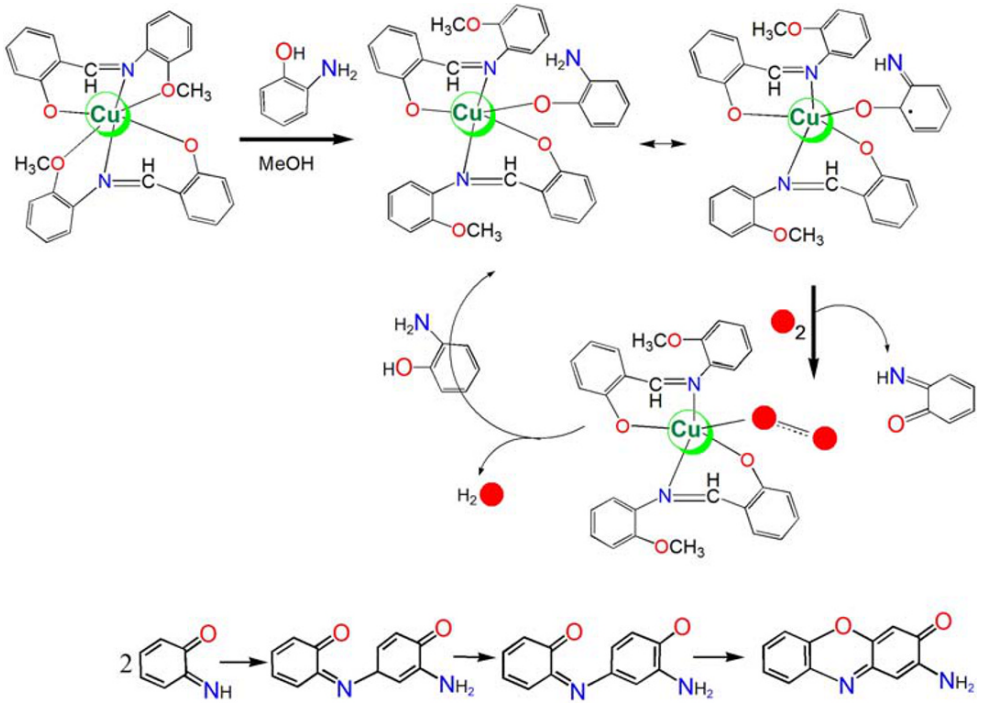

SCHEME 3 Plausible mechanism for the catalytic oxidation of 2-AP

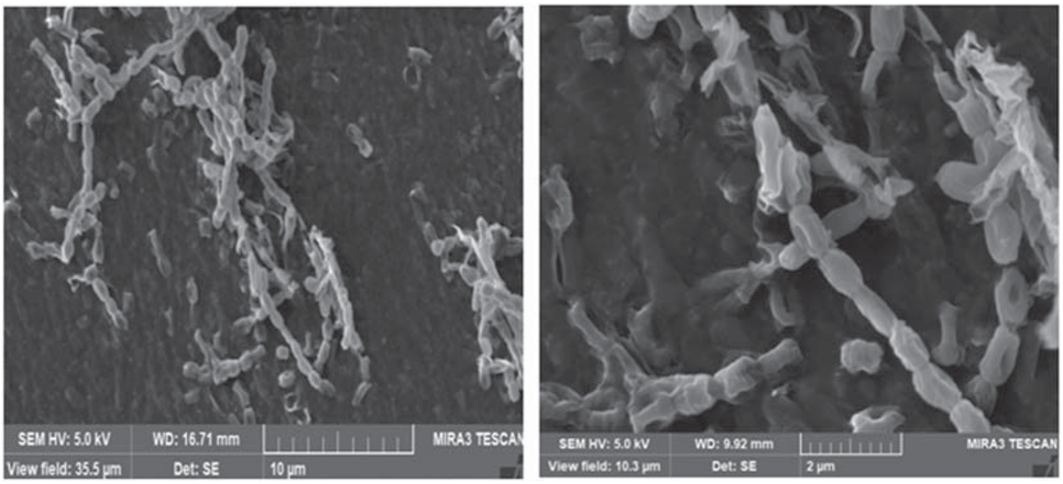

FIGURE 5 Electron microscope scans showing morphological changes in pathogenic bacteria. Destruction of the bacterial cell membrane (MIC) and B growth of bacteria (MBC)

this Cu (II)-Schiff base complex. Scientific literatures suggest that the Cu (II) complex is quite competent to inhibit the growth of pathogenic bacterial species. Aiming to explore the origin of antibacterial property for this copper (II)-Schiff base complex, a study involving the exposure of Cu (II) complex on *Klebsiella pneumoniae* was carried out employing scanning electron microscope (SEM) analysis. SEM image of the *Klebsiella pneumoniae* in presence of Cu (II) complex accounts on the change of morphology on the cell wall. The recorded SEM micrographs of *Klebsiella pneumonia* cells are shown in Figure 5.

Commonly, MBC of *Klebsiella pneumonia* was observed as typical rod-shape with smooth and intact cell walls. Although, the number of *Klebsiella pneumonia* was remarkably decreased, and cell walls became wrinkled and damaged after addition of Cu (II) complex to *Klebsiella pneumonia.*[50,51] In reality, in limited cases, such type of observations were noted and will definitely bring some hope in developing suitable therapeutic agents.

4 | CONCLUSIONS

This research study provides an overview of synthesis, X-ray structural characterization, Hirshfeld surface analysis and bio-mimetic oxidation of 2-AP as well as antibacterial activity of a newly synthesized copper (II)-Schiff base complex, $[Cu(\mathbf{L})_2]$ (**1**). X-ray structure of the Cu (II) complex shows that the Cu (II) centre adopts an unprecedented tetragonal bipyramidal geometry in its crystalline phase. The copper (II) complex has been evaluated as a bio-inspired catalyst towards oxidative coupling of 2-AP in acetonitrile and exhibits good catalytic activity with turnover number, 536.4 h^{-1}. In view of mechanistic insights, electrochemical analysis of the Cu (II) complex in presence of 2-AP was carried out and indicates the generation of $AP^{-}/AP^{\bullet -}$ and $AP^{\bullet -}/IQ$ redox couple in the course of catalysis. EPR spectral analysis of the reaction mixture confirms the existence iminobenzosemiquinone radical at g = 2.057 which suggests the radical driven catalytic oxidation of 2-AP. Furthermore, ESI-MS analysis of the Cu (II) complex in presence of 2-AP ensures that the catalytic oxidation of 2-AP proceeds through the formation of enzyme-substrate adduct. Antibacterial property of the copper (II) complex has been examined against different pathogenic bacteria. Scanning electron microscope images reveal that destruction of bacterial cell membrane remains the driving force for the development of potential antibacterial properties of the copper (II)-Schiff base complex. Importantly, this Schiff base ligand can able to isolate Cu (II) ion in an intermediate coordination geometry (tetragonal bipyramidal geometry) and represents a rare example of unprecedented coordination geometry which is controlled by steric factors of the Schiff base ligand.

ACKNOWLEDGEMENTS

BB sincerely acknowledges Science and Engineering Research Board (SERB), India for financial support under TEACHERS' ASSOCIATESHIP for RESEARCH EXCELLENCE (TAR/2018/000473). MJ thanks DST INSPIRE Programme for research fellowship. ARC thanks Department of Chemical Sciences, IISER Mohali for X-ray facility.

ORCID

Bhaskar Biswas https://orcid.org/0000-0002-5447-9729

REFERENCES

[1] Y. Ruan, X. Jia, C. Wang, W. Zhen, X. Jiang, *ACS Biomater. Sci. Eng.* **2019**, *5*, 1016.
[2] A. S. Smirnov, L. M. D. R. S. Martins, D. N. Nikolaev, R. A. Manzhos, V. V. Gurzhiy, A. G. Krivenko, K. O. Nikolaenko, A. V. Belyakov, A. V. Garabadzhiu, P. B. Davidovich, *New J. Chem.* **2019**, *43*, 188.
[3] W. Al Zoubi, Y. G. Ko, *Appl. Organomet. Chem.* **2016**, *31*, e3574.
[4] D.-D. Li, E. Yagüe, L.-Y. Wang, L.-L. Dai, Z.-B. Yang, S. Zhi, N. Zhang, X.-M. Zhao, Y.-H. Hu, *ACS Med. Chem. Lett.* **2019**, *9*, 1328.
[5] X. Li, K. Du, J. Sun, F. Feng, *ACS Appel. Bio. Mat.* **2020**, *3*, 654.
[6] M. K. Ghosh, S. Pathak, T. K. Ghorai, *ACS Omega* **2019**, *4*, 16068.
[7] Y. Fan, J. Zhang, M. Shi, D. Li, C. Lu, X. Cao, C. Peng, S. Mignani, J.-P. Majoral, X. Shi, *Nano Lett.* **2019**, *19*, 1216.
[8] E. I. Solomon, D. E. Heppner, E. M. Johnston, J. W. Ginsbach, J. Cirera, M. Qayyum, M. T. Kieber-Emmons, C. H. Kjaergaard, R. G. Hadt, L. Tian, *Chem. Rev.* **2014**, *114*, 3659.
[9] E. I. Solomon, M. J. Baldwin, M. D. Lowery, *Chem. Rev.* **1992**, *92*, 521.
[10] (a) E. I. Solomon, B. L. Hemming, D. E. Root, *Electronic Structures of Active Sites in Copper Proteins: Coupled Binuclear and Trinuclear Cluster Sites in Bioinorganic chemistry of copper*, (K. D. Karlin, Z. Tyeklár), Chapman & Hall Publishing House, New York, USA, **1993**, doi:https://doi.org/10.1007/978-94-011-6875-5
[11] C. Mukherjee, U. Pieper, E. Bothe, V. Bachler, E. Bill, T. Weyhermüller, P. Chaudhuri, *Inorg. Chem.* **2008**, *47*, 8943.
[12] (a) J.L. McLain, J. Lee, J. T. Groves, in *Biomimetic Oxidations Catalyzed by Transition Metal Complexes*, (Ed.: Meunier B.), Imperial College Press, London; (b) F. Benedini, G. Galliani, M. Nali, B. Rindone, S. Tollari, *J. Chem. Soc. Perkin Trans.* **1985**, *2*, 1963; (c) K. D. Karlin, Z. Tyeklár, A. Farooq, M. S. Haka, P. Ghosh, R. W. Cruse, Y. Gultneh, J. C. Hayes, P. J. Toscano, J. Zubieta, *Inorg. Chem.* **1991**, *31*, 1436.
[13] (a) L. I. Simándi, S. Németh, N. Rumlis, *J. Mol. Catal.* **1987**, *42*, 357; (b) Z. Szeverenyl, E. R. Mileava, L. I. Simándi, *J. Mol. Catal.* **1991**, *67*, 251; (c) G. C. Paul, K. Das, S. Maity, S. Begum, H. K. Srivastava, C. Mukherjee, *Inorg. Chem.* **2018**, *58*, 1782.
[14] (a) S. Dutta, J. Mayans, A. Ghosh, *Dalton Trans.* **2020**, *49*, 1276; (b) A. Begum, A. H. Sheikh, G. Moula, S. Sarkar, *Sci. Rep.* **2017**, *7*, 1; (c) B. Mondal, A. Dey, *Chem. Commun.* **2017**, *53*, 7707; (d) I. Ghosh, S. Banerjee, S. Paul, T. Corona, T. K. Paine, *Angew. Chem., Int. Ed.* **2019**, *58*, 12534; (e) A. Sarkar, A. Chakraborty, A. Adhikary, S. Maity, A. Mandal, D. Samanta, P. Ghosh, D. Das, *Dalton Trans.* **2019**, *48*, 14164.
[15] (a) N. C. Jana, M. Patra, P. Brandão, A. Panja, *Inorg. Chim. Acta* **2019**, *490*, 163; (b) S. Thakur, S. Banerjee, S. Das, S. Chattopadhyay, *New J. Chem.* **2019**, *43*, 18747; (c) M. Garai, D. Dey, H. R. Yadav, A. R. Choudhury, M. Maji, B. Biswas, *ChemistrySelect* **2017**, *2*, 11040; (d) A. De, M. Garai, H. R. Yadav, A. R. Choudhury, B. Biswas, *Appl. Organomet. Chem.* **2017**, *31*, e3551.
[16] (a) C. C. L. McCrory, S. Jung, I. M. Ferrer, S. M. Chatman, J. C. Peters, T. F. Jaramillo, *J. Am. Chem. Soc.* **2015**, *137*, 4347; (b) D. Li, H. Baydoun, C. N. Verani, S. L. Brock, *J. Am. Chem. Soc.* **2016**, *138*, 4006.
[17] S. Sakaue, T. Tsubakino, Y. Nishiyama, Y. Ishii, *J. Org. Chem.* **1993**, *58*, 3633.
[18] J. Kaizer, R. Csonka, G. Speier, *J. Mol. Catal. A: Chem.* **2002**, *180*, 91.
[19] T. Horváth, J. Kaizer, G. Speier, *J. Mol. Catal. A: Chem.* **2004**, *215*, 9.
[20] M. R. Maurya, S. Sikarwar, T. Joseph, S. B. Halligudi, *J. Mol. Catal. A: Chem.* **2005**, *236*, 132.
[21] K. Anzai, K. Isono, K. Ohkuma, S. Suzuki, *J. Antibiot.* **1960**, *13*, 125.
[22] A. Iwata, T. Yamaguchi, K. Sato, R. Izumi, A. Tomoda, *Tohoku J. Exp. Med.* **2003**, *200*, 161.
[23] Y. Igarashi, K. Takagi, T. Kajiura, T. Furumai, T. Oki, *J. Antibiot.* **1998**, *51*, 915.
[24] T. Schimamoto, A. Tomoda, R. Ishida, K. Ohyashiki, *Clin. Cancer Res.* **2001**, *7*, 704.
[25] S. Shimizu, M. Suzuki, A. Tomoda, S. Arai, H. Taguchi, T. Hanawa, S. Kamiya, *Tohoku J. Exp. Med.* **2004**, *203*, 47.
[26] (a) P. Dorrestein, T. P. Begley, *Bioorg. Chem.* **2005**, *33*, 136; (b) P. Mahapatra, S. Ghosh, S. Giri, V. Rane, R. Kadam, M. G. B. Drew, A. Ghosh, *Inorg. Chem.* **2017**, *56*, 5105; (c) P. K. Mudi, N. Bandopadhyay, M. Joshi, M. Shit, S. Paul, A. R. Choudhury, B. Biswas, *Inorg. Chim. Acta* **2020**, *505*; 119468.
[27] C. Eggert, *Microbiol. Res.* **1997**, *152*, 315.
[28] M. A. Hughes, M. J. Baggs, J. Al-Dulayymi, M. S. Baird, P. A. Williams, *Appl. Environ. Microbiol.* **2002**, *68*, 4965.
[29] C. Duncan, A. R. White, *Metallomics* **2012**, *4*, 127.
[30] J. Zhang, D. Duan, J. Xu, J. Fang, *ACS Appl. Mat. Interfer.* **2018**, *10*, 33010.
[31] K. Y. Djoko, M. M. Goytia, P. S. Donnelly, M. A. Schembri, W. M. Shafer, A. G. McEwan, *Antimicrob. Agents Chemother.* **2015**, *59*, 6444.
[32] (a) M. Garai, A. Das, M. Joshi, S. Paul, M. Shit, A. R. Choudhury, B. Biswas, *Polyhedron* **2018**, *156*, 223; (b) D. Dey, G. Kaur, A. Ranjani, L. Gayathri, P. Chakraborty, J. Adhikary, J. Pasan, D. Dhanasekaran, A. R. Choudhury, M. A. Akbarsha, N. Kole, B. Biswas, *Eur. J. Inorg. Chem.* **2014**, *2014*, 3350; (c) D. Dey, G. Kaur, M. Patra, A. R. Choudhury, N. Kole, B. Biswas, *Inorg. Chim. Acta* **2014**, *421*, 335; (d) C. K. Pal, S. Mahato, M. Joshi, S. Paul, A. R. Choudhury, B. Biswas, *Inorg. Chim. Acta* **2020**, *506*, 119541.
[33] (a) CrysAlisPro 1.171.39.35c, (**2017**) Rigaku Oxford Diffraction, *Rigaku Corporation*: Tokyo, Japan; (b) G. M. Sheldrick, *Acta Cryst.* **2015**, *A71*, 3; (c) G. M. Sheldrick, *Acta Cryst.* **2015**, *C71*, 3; (d) O. V. Dolomanov, L. J. Bourhis, R. J. Gildea, J. A. K. Howard, H. Puschmann, *J. Appl. Cryst.* **2009**, *42*, 339.
[34] (a) M. J. Turner, J. J. McKinnon, S. K. Wolff, D. J. Grimwood, P. R. Spackman, D. Jayatilaka, M. A. Spackman, Crystal Explorer, University of Western Auestralia, http://hirshfeldsurface.net17 (**2017**); (b) M. A. Spackman, D. Jayatilaka, *CrystEngCom.* **2009**, *11*, 19; (c) S. K. Seth, V. S. Lee, J. Yana, S. M. Zain, A. C. Cunha, V. F. Ferreira, A. K. Jordao, M. C. B. V. de Souza, S. M. S. V. Wardell, J. L. Wardellf, E. R. T. Tiekink, *Cryst. Eng. Comm.* **2015**, *17*, 2255; (d) M. N. Ahamad, M. Kumar, A. Ansari, I. Mantasha, M. Ahmad, M. Shahid, *New J. Chem.* **2019**, *43*, 14074.

[35] (a) M. A. Spackman, D. Jayatilaka, *Cryst. Eng. Comm.* **2009**, 1119; (b) M. A. Spackman, J. J. McKinnon, *Cryst. Eng. Comm.* **2002**, *4*, 378.
[36] H. Yamatera, *Acta Chem. Scand. A* **1979**, *33*, 107.
[37] C. K. Pal, S. Mahato, H. R. Yadav, M. Shit, A. R. Choudhury, B. Biswas, *Polyhedron* **2019**, *174*, 114156.
[38] D. Dey, S. Das, H. R. Yadav, A. Ranjani, L. Gyathri, S. Roy, P. S. Guin, D. Dhanasekaran, A. R. Choudhury, M. A. Akbarsha, B. Biswas, *Polyhedron* **2016**, *106*, 106.
[39] A. Anwar, A. Masri, K. Rao, K. Rajendran, N. A. Khan, M. R. Shah, R. Siddiqui, *Sci. Rep.* **2019**, *9*, 3122.
[40] F. M. W. Nongkhlaw, S. R. Joshi, *J. Microsc. Ultrastruct.* **2017**, *5*, 132.
[41] B. Chowdhury, M. Karar, S. Paul, M. Joshi, A. R. Choudhury, B. Biswas, *Sens. Actuators, B* **2018**, *276*, 560.
[42] (a) A. De, D. Dey, H. R. Yadav, M. Maji, V. Rane, R. M. Kadam, A. R. Choudhury, B. Biswas, *J. Chem. Sci.* **2016**, *128*, 1775; (b) S. Khan, S. Herrero, R. González-Prieto, M. G. B. Drew, S. Banerjee, S. Chattopadhyay, *New J. Chem.* **2018**, *42*, 13512; (c) T. M. Rajendiran, R. Kannappan, R. Mahalakshmy, J. Rajeswari, R. Venkatesan, P. Rao, *Transition Met. Chem.* **2003**, *28*, 447.
[43] W. J. Geary, *Coord. Chem. Rev.* **1971**, *7*, 81.
[44] B. Chowdhury, B. Bhowmik, A. Sahu, M. Joshi, S. Paul, A. R. Choudhury, B. Biswas, *J. Chem. Sci* **2018**, *130*, 161.
[45] A. K. Ghosh, A. Ali, Y. Singh, C. S. Purohit, R. Ghosh, *Inorg. Chim. Acta* **2018**, *474*, 156.
[46] S. Sagar, S. Sengupta, A. J. Mota, S. K. Chattopadhyay, A. E. Ferao, E. Riviere, W. Lewis, S. Naskar, *Dalton Trans.* **2017**, *46*, 1249.
[47] B. Chowdhury, M. Maji, B. Biswas, *J. Chem. Sci.* **2017**, *129*, 1627.
[48] C. Mukherjee, T. Weyhermüller, E. Bothe, E. Rentschler, P. Chaudhuri, *Inorg. Chem.* **2007**, *46*, 9895.
[49] (a) C. E. Barry III, P. G. Nayar, T. P. Begley, *Biochemistry* **1989**, *28*, 6323; (b) C. E. Barry III, P. G. Nayar, T. P. Begley, *J. Am. Chem. Soc.* **1988**, *110*, 3333; (c) J. C. Freeman, P. G. Nayar, T. P. Begley, J. J. Villafranca, *Biochemistry* **1993**, *32*, 4826.
[50] A. Reyes-Jara, N. Cordero, J. Aguirre, M. Troncoso, G. Figueroa, *Front. Microbiol.* **2016**, *7*.
[51] H. Li, Q. Chen, J. Zhao, K. Urmila, *Sci. Rep.* **2015**, *5*.

SUPPORTING INFORMATION

Additional supporting information may be found online in the Supporting Information section at the end of this article.

How to cite this article: Mahato S, Meheta N, Kotakonda M, et al. Ligand directed synthesis of a unprecedented tetragonalbipyramidal copper (II) complex and its antibacterial activity and catalytic role in oxidative dimerisation of 2-aminophenol. *Appl Organomet Chem*. 2020;e5935. https://doi.org/10.1002/aoc.5935